



Cite this: *Phys. Chem. Chem. Phys.*,
2018, 20, 3381

"*In situ*" observation of the role of chloride ion binding to monkey green sensitive visual pigment by ATR-FTIR spectroscopy†

Kota Katayama,^a Yuji Furutani,^b Masayo Iwaki,^a Tetsuya Fukuda,^a Hiroo Imai^c and Hideki Kandori^{ib} *^{ad}

Long-wavelength-sensitive (LWS) pigment possesses a chloride binding site in its protein moiety. The binding of chloride alters the absorption spectra of LWS; this is known as the chloride effect. Although the two amino acid substitutions of His197 and Lys200 influence the chloride effect, the molecular mechanism of chloride binding, which underlies the spectral tuning, has yet to be clarified. In this study, we applied ATR-FTIR spectroscopy to monkey green (MG) pigment to gain structural information of the chloride binding site. The results suggest that chloride binding stabilizes the β -sheet structure on the extracellular side loop with perturbation of the retinal polyene chain, promotes a hydrogen bonding exchange with the hydroxyl group of Tyr, and alters the protonation state of carboxylate. Combining with the results of the binding analyses of various anions (Br^- , I^- and NO_3^-), our findings suggest that the anion binding pocket is organized for only Cl^- (or Br^-) to stabilize conformation around the retinal chromophore, which is functionally relevant with absorbing long wavelength light.

Received 27th October 2017,
Accepted 19th December 2017

DOI: 10.1039/c7cp07277e

rsc.li/pccp

Vertebrate cone pigments are classified into four classes on the basis of their primary sequence and spectral properties (λ_{max}): S (SWS1, $\lambda_{\text{max}} = 415$), M1 (SWS2, $\lambda_{\text{max}} = 455$), M2 (Rh2, $\lambda_{\text{max}} = 508$), and L (LWS, $\lambda_{\text{max}} = 571$).¹ All pigments possess a common chromophore, 11-*cis*-retinal, which is attached by a Schiff-base linkage to a protein moiety. However, 11-*cis*-retinal enables cone pigments to detect/absorb a wide range of wavelengths through a specific interaction with the protein moiety. This unique phenomenon, involving the interaction of a common chromophore and various visual pigments, results in a wide spectral-width and is termed as an opsin shift.^{2,3} In addition, it is well known that cone pigments in the L group have a chloride (Cl^-) binding site in their protein moieties and shift the absorption maxima to a longer wavelength (~ 40 nm). Previous studies revealed His197 and Lys200 to contribute to Cl^- -binding and that His197 is the primary residue for the Cl^- effect.⁴ The crystal structure of bovine Rh revealed that these sites are located in the second extracellular loop (ECL2), which

forms a β -sheet structure and is close to the Cys203(45.50)–Cys126(3.25) (the numbers in parenthesis denote the residue position in the Ballesteros–Weinstein scheme⁵) disulfide bond linking the luminal end of Helix3.⁶ Therefore, the Cl^- binding site is strongly suggested to be in the vicinity of the retinal Schiff base. However, the structural basis underlying the binding mechanism of Cl^- and its effect on spectral tuning is poorly understood due to the unavailability of structural studies on cone pigments.

Previously, we succeeded in structural analysis of monkey red (MR) and green (MG) pigments by using low-temperature FTIR spectroscopy, from which we revealed important structural differences, such as MG specific amide-I vibration, MR specific X–H stretch,⁷ and unique hydrogen bonded internal water molecules in both MR and MG.⁸ In particular, strong hydrogen-bonded water molecules were observed for both MR and MG after formation of the batho-intermediate state, which was not observed in case of Rh⁹ and monkey blue (MB) pigment.¹⁰ Presumably, these water molecules would participate in the Cl^- binding site near the retinal chromophore. Since low-temperature FTIR spectroscopy requires the protein samples as a hydrated film at 77 K, "*in situ*" detection of structural change induced by the ion binding is challenging due to the restrictions on molecular interactions at such low temperatures.

To characterize the functional role of Cl^- in the L group pigments, we studied specific interactions of Cl^- with MG-pigment using attenuated total reflection (ATR)-FTIR difference spectroscopy.

^a Department of Life Science and Applied Chemistry, Nagoya Institute of Technology, Showa-ku, Nagoya 466-8555, Japan. E-mail: kandori@nitech.ac.jp

^b Department of Life and Coordination-Complex Molecular Science, Institute for Molecular Science, 38 Nishigo-Naka, Myodaiji, Okazaki 444-8585, Japan

^c Primate Research Institute, Kyoto University, Inuyama 484-8506, Japan

^d OptoBio Technology Research Center, Nagoya Institute of Technology, Showa-ku, Nagoya 466-8555, Japan

† Electronic supplementary information (ESI) available. See DOI: 10.1039/c7cp07277e

The ATR mode allows the measurement of vibrational signals from the evanescent field and minimizes contribution from the water background. This technique has been widely used to investigate the structural changes of membrane proteins induced by ligand (ion or substrate) binding.^{11–13} In this study, Cl[−]-binding-induced structural change of MG-pigment was detected, which enabled us to identify the region that binds to the Cl[−] and its subsequent effect on the protein conformation.

Results

Cl[−]-Binding-induced difference ATR-FTIR spectroscopy of monkey green (MG) sensitive visual pigment at physiological condition

Fig. S1 (ESI[†]) shows the absolute infrared absorption spectrum of MG-pigment adsorbed onto the ATR crystal and Fig. 1a shows the Cl[−]-binding-induced difference infrared spectrum measured in the buffer containing 200 mM phosphate (pH 7.25) and 10 mM NaCl against the buffer without NaCl as reference. The dissociation constant (K_d) reported for Cl[−]-binding is 0.1 mM for iodopsin,¹⁴ which is 100-fold lower in concentration than that in our experimental conditions. Therefore, the spectral changes observed in Fig. 1 are representative of a fully occupied binding site. In fact, a similar Cl[−]-binding spectrum was obtained at 25 mM NaCl condition (see Fig. S2, ESI[†]). Cl[−] perfusion-induced difference FTIR spectroscopic analysis has been already reported for Halorhodopsin from *Natronomonas pharaonis* (NpHR), a light-driven Cl[−] pump^{15,16} used to investigate the anion transport mechanism during the photocycle and spectral tuning from the anion free form (blue NpHR) to the anion bound form

(NpHR576) (see Fig. S3 black line, ESI[†]). In Fig. S3 (ESI[†]), the pair bands at 1525(+)/1511(−) cm^{−1} correspond to C=C stretching vibration band of retinal chromophore, which is consistent with a blue shift in λ_{\max} .¹⁵ Furthermore, the pair bands at 1674(−)/1658(+) cm^{−1} may correspond to local structural perturbation of α -helix induced by Cl[−]-binding.

In the present measurement (see Fig. 1a and Fig. S3 red line, ESI[†]), the pair bands at 1547(−)/1532(+) cm^{−1} correspond to a C=C stretching vibration of the retinal chromophore, and down-shift with Cl[−]-binding is consistent with red-shift in the visible region. Along with the vibrational bands of NpHR, Cl[−]-binding-induced polypeptide backbone alterations are evident from several vibrational bands in the amide-I region, that is, binding and/or dissociation of Cl[−] also provides MG-pigment perturbation of the α -helix. It should be noted that a dominant positive band appears at 1620 cm^{−1}. This band frequency corresponds to an amide-I vibrational mode of a typical β -sheet. Moreover, it is well known that C–C stretching vibrations of the retinal chromophore appear at around 1200 cm^{−1}. In Fig. S4 (ESI[†]), we could identify the bands at 1197 cm^{−1} as one of the C–C stretching vibrations of the retinal chromophore as observed during the measurements of 9-*cis*-retinal bound form of MG-pigment, where the band is shifted from 1197 to 1206 cm^{−1} (Fig. S4b, ESI[†]). This band could be assigned to the C₁₄–C₁₅ stretching vibration.¹⁷ Although conventional light-induced difference FTIR spectra have been intensively examined to identify the vibrational bands by use of isotope labeling and site-directed mutation, ATR-FTIR spectra still lag far behind as a means of explaining the structural changes based on the vibrational bands in the difference spectra.

Amino acids hydrogen–deuterium exchange ATR-FTIR spectroscopy of MG-pigment

To investigate the origins of vibrational bands observed in a difference spectrum, an H/D exchange experiment was performed in D₂O media (Fig. 1b, red line). As shown in Fig. 1b, the 1231 cm^{−1} band exhibited up-shift to 1239 cm^{−1} (see Fig. S5b, ESI[†]), suggesting that the band originated from the C–O stretching vibration of a Tyr residue although some vibrational bands exhibited down-shift in D₂O. The hydroxyl group of Tyr can take four different bond forms, *i.e.*, free, hydrogen-bond donor, acceptor, and donor–acceptor forms, and each hydrogen-bond form provides a different vibrational mode in the following frequency regions: 1260–1250, 1280–1260, 1240–1220, and 1255–1235 cm^{−1}.¹⁸ Thus, the Tyr side chain with 1231 cm^{−1}-band would play the role of a hydrogen bond acceptor for Cl[−]-binding (Fig. 1b).

As shown in Fig. 1b, small down-shifts were observed in the 1700–1600 cm^{−1} region in D₂O, relative to H₂O, as expected for amide-I bands. The β -sheet specific amide-I bands at 1620(+)/1695(+) cm^{−1} are slightly down-shifted in D₂O relative to H₂O, *i.e.*, by 5 and 3 cm^{−1}, respectively. The range of band shift is consistent with the previous report.¹⁹ It should be noted that the positive band corresponding to the Cl[−] bound form is predominant, suggesting that Cl[−]-binding might relate to the structural stability of MG-pigment, particularly in the

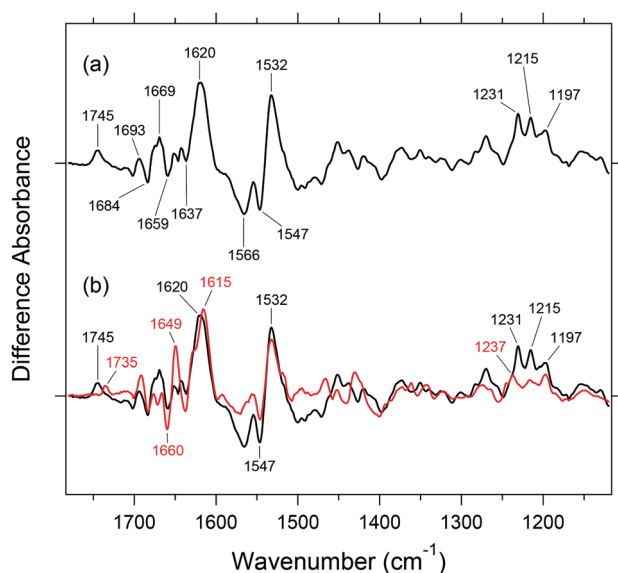


Fig. 1 (a) The ion-binding induced difference FTIR spectrum of MG. The difference spectrum was measured in the presence and absence of 10 mM NaCl at room-temperature in the 1780–1120 cm^{−1} region. (b) The ion-binding induced difference FTIR spectrum in H₂O (black curve at pH 7.25) and D₂O (red curve at pD 7.25) of MG. One division of the y-axis corresponds to 0.001 absorbance unit.

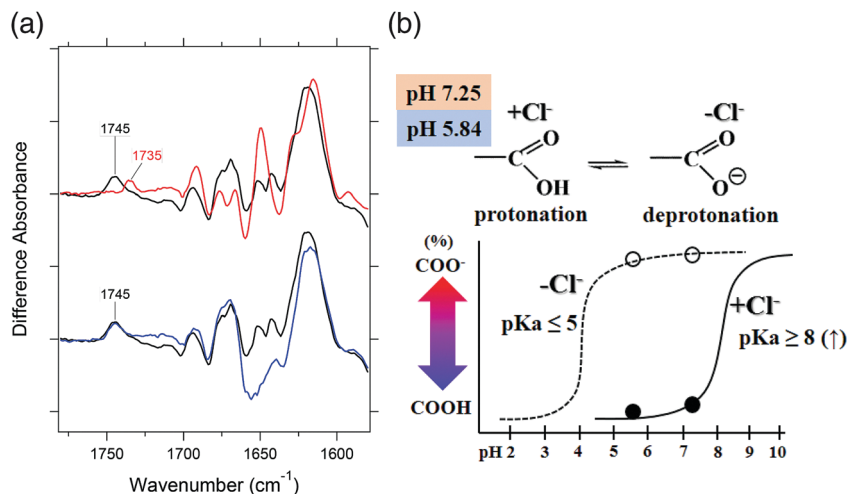


Fig. 2 (a) The ion-binding induced difference FTIR spectra of MG. Upper panel: Cl^- -minus-anion free difference spectra in H_2O (black curve) and D_2O (red curve) in the $1780\text{--}1550\text{ cm}^{-1}$ region. Lower panel: Cl^- -minus-anion free difference spectra in pH 7.25 (black curve) and pH 5.84 (blue curve) in the $1780\text{--}1550\text{ cm}^{-1}$ region. One division of the y-axis corresponds to 0.0002 absorbance unit. (b) The ideal model traces of pH titration for a carboxylate group in the presence (solid line) and absence (dashed line) of Cl^- . Y-axis shows the population of protonated and/or deprotonated state of a carboxyl group, and x-axis shows the pH values.

β -sheet structure. In fact, recent mutagenesis studies of His197 on *Macaca fascicularis* green cone visual pigment (mfasc green) indicated that the presence of a histidine residue at this position could result in increased stability of the β -sheet.²⁰

The positive band at 1745 cm^{-1} is shifted to 1735 cm^{-1} due to H/D exchange effects. Fig. 2a represents an expansion of the $1750\text{--}1730\text{ cm}^{-1}$ region (Fig. 1b). The bands originating from a protonated carboxyl group, observed in H_2O (black curve) and in D_2O (red curve), are slightly sharp without a shoulder band. Indeed, these bands are well fitted by only one-component of Gaussian distribution (Fig. S6 bold curve, ESI†). This may indicate that one carboxyl group contributes to form the Cl^- binding site in the ECL2 of MG-pigment. Notably, the negative band does not appear in the $\text{C}=\text{O}$ stretching vibration region of protonated carboxyl groups, suggesting that this carboxylate can be protonated upon Cl^- -binding and, in contrast, deprotonated by the Cl^- dissociation. However, a counterpart band as a deprotonated $\text{C}=\text{O}$ stretching vibration is not confirmed around 1400 cm^{-1} region due to the overlap of several bands. The protonation of carboxylate induced by Cl^- -binding also occurs in *pharaonis* phorbodopsin (ppR, sensory rhodopsin II (pSRII)).²¹ To examine the effect of protonation in detail, pH dependent experiment was performed, in which the acidic pH may contribute to protonation of the carboxylate both in the presence and absence of Cl^- (Fig. 2a, blue curve). Even at pH 5.84, the positive band at 1745 cm^{-1} was unaltered, indicating that pK_a value of Cl^- bound form is more than 8.0, while that of the Cl^- unbound form is less than 5.0 in the solution. This indicates that the pK_a of the carboxyl group would be elevated considerably by binding of Cl^- (Fig. 2).

Taking into account of the X-ray crystal structure of Rh, one strong candidate for this carboxyl group is Asp206, which is located on the ECL and can form an ion-pair with Arg193. Remarkably, this ion-pair is conserved among most opsins including

cone pigments, and Asp206 mutations have been observed in several cases of *retinitis pigmentosa*.^{22–24} It was reported that mutations on the ion-pair either result in opsin proteins that do not bind to 11-*cis*-retinal or, if they do regenerate, undergo rapid retinal Schiff base hydrolysis in the dark state.^{25,26} Therefore, this ion-pair would be affected by binding of Cl^- in the case of cone pigments in terms of stabilization, which results in rearrangement for more optimized structural formation.

Comparison of each anion-binding-induced difference ATR-FTIR spectroscopy of MG-pigment

The Cl^- binding site is not specific to Cl^- and can accommodate different monovalent anions, including nitrate, perchlorate, and thiocyanate.^{27,28} Thus, it is valuable to investigate the difference in the binding mechanisms of several types of anions based on the structural information. Fig. 3 shows the comparison of four types of anion binding-induced difference FTIR spectra. As shown in the red curve in Fig. 3b, the nitrate binding-induced difference FTIR spectrum exhibits α -helix specific amide-I pair bands at $1658(-)/1649(+)\text{ cm}^{-1}$, while vibrational bands originating from β -sheet or retinal chromophore do not appear as compared to the spectrum of the Cl^- bound form (black curve). This result strongly suggests that nitrate can also bind, but not in the vicinity of the retinal polyene chain. In fact, the spectral feature of Cl^- -minus- NO_3^- (Fig. 3c, red curve) closely resembles the Cl^- -minus-anion free spectrum (Fig. 3c, black curve) except for the amide-I band region. The pair bands at $1658(-)/1649(+)\text{ cm}^{-1}$, which are located in the amide-I region specific to α -helix, would originate from an α -helix, suggesting the nitrate binding-induced structural perturbation on an α -helix in the extracellular side. Moreover, the signal intensity of the amide-I band specific to β -sheet in the Cl^- -minus- I^- difference spectrum (Fig. 3d, red curve) decreased, although the overall spectral feature was quite similar to that of Cl^- -minus-anion

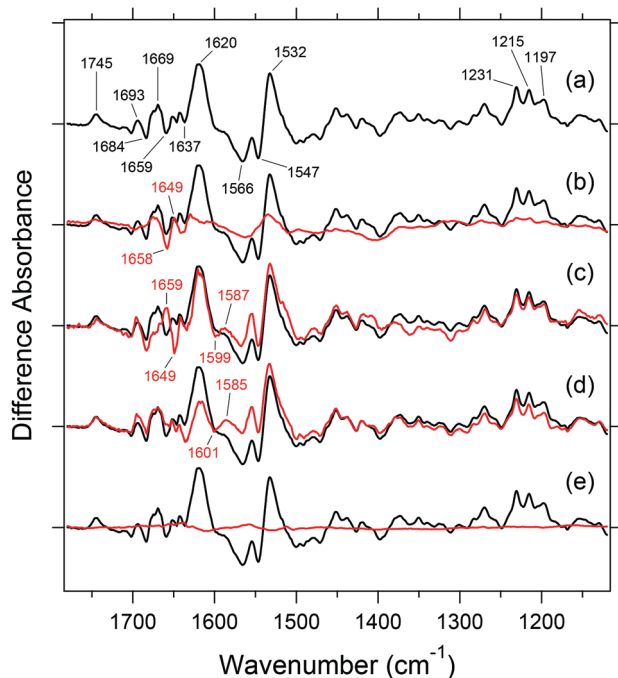


Fig. 3 The comparison of ion-binding induced difference FTIR spectra of MG. Each black spectrum corresponds to Cl^- -minus- anion free difference spectra in the $1780\text{--}1120\text{ cm}^{-1}$ region. Red spectrum in (b) corresponds to difference between nitrate (10 mM) and anion free. Red spectrum in (c) corresponds to difference between Cl^- and nitrate. Red spectrum in (d) corresponds to difference between Cl^- and I^- . Red spectrum in (e) corresponds to difference between Cl^- and Br^- . One division of the y-axis corresponds to 0.0005 absorbance unit.

free (Fig. 3d, black curve). This may indicate that binding of I^- also contributes to the β -sheet structural stability, similar to the Cl^- bound form. In contrast, there is no structural alteration between Cl^- and Br^- -binding forms (Fig. 3e, red curve), strongly indicating the same binding manner for both ions. Therefore, these results suggest that the anion binding pocket accommodates Cl^- and Br^- , but not I^- or NO_3^- which cannot interact with the protein moiety like Cl^- (or Br^-).

Discussion

The binding of Cl^- induces several polypeptide backbone changes in MG, particularly in its β -sheet structure, perturbation of the retinal polyene chain, changes in the hydrogen bonding network of a hydroxyl group of Tyr, and the alteration of protonation state of carboxyl group. The positive 1620 cm^{-1} band corresponds to the β -sheet-specific amide-I band. Appearance of this band may indicate that Cl^- -binding possibly contributes to the structural stability of MG-pigment, which is in agreement with the recent mutagenesis study²⁰ reporting that the presence of Cl^- is able to enhance the formation of the β -sheet. The band located at 1197 cm^{-1} , probably originating from the $\text{C}_{14}\text{--}\text{C}_{15}$ stretching vibration of the retinal chromophore, would be affected by Cl^- -binding coupled with the hydrogen bonding change of Tyr (probably Tyr284(6.51)), whose C–O stretching mode was observed as the positive 1231 cm^{-1} band because the

location of Tyr284(6.51) is close to $\text{C}_{14}\text{--}\text{C}_{15}$ according to the X-ray crystal structure of Rh. In addition, this hydrogen bonding change would cause perturbation in internal water molecules. Cl^- or other monovalent anions can form hydration structures in the bulk water to stabilize their negative charge. This hydration energy partly depends on the strength of interaction between an anion and water molecules since hydrated interaction is explained by a typical ion–dipole interaction.²⁹ Moreover, the hydration structure of an anion inside a protein can be different compared with that in bulk water; thus, partial or complete dehydration may occur inside the protein. Previously, we found a strongly hydrogen bonded water molecule, which changes its structure after photoisomerization of retinal only in MR and MG, but not in Rh and MB, using light-induced difference FTIR spectroscopy.^{8–10} In the previous studies on pHR²⁸ and cone pigments,⁸ we discussed Cl^- being weakly hydrated by internal water, but photoisomerization perturbs the local structure of the binding site, resulting in formation of a strong H-bond with water. Hence, one would come up with a speculation that partial dehydration of Cl^- occurs upon its binding in the vicinity of the retinal chromophore, but the Cl^- still can interact with a hydrophilic amino acid having a dipole moment (one candidate is Tyr284(6.51)) as compensation for loss of hydration energy.

In addition, Cl^- -binding-induced structural changes in protein are possibly accompanied by the protonation change of a carboxyl group, whose C=O stretching band was observed at 1745 cm^{-1} . One possible candidate of this carboxyl group is Asp206 as reference of Rh structure. Asp206 can form an ion-pair with Arg193 on the ends of ECL. This ion-pair (Arg193/Asp206) is conserved in almost all vertebrate opsins and might be present in other GPCRs as well. In addition, mutations at Asp206 in Rh are found in patients with Autosomal Dominant Retinitis Pigmentosa (ADRP).^{22–24} However, it should be noted that this disease is related to rhodopsin mutation and not to cone pigments, so the functional role of this ion-pair between rod and cone pigments may be different. From the present results, this ion-pair is affected by binding of Cl^- in the case of cone pigments in terms of stabilization, which induces rearrangement for more optimized structural formation.

It has been assumed that the chloride binding site in cone pigments accommodates various monovalent anions as well as Cl^- including a relatively large anion such as nitrate. However, the nitrate bound form exhibits $\sim 40\text{ nm}$ blue shift in the absorption maximum compared to that of the Cl^- bound form in the case of iodopsin.³⁰ From the present anion exchange induced difference FTIR spectra, however, it was elucidated that the I^- or NO_3^- -binding forms can induce perturbation to α -helix and/or β -sheet while there is no structural alteration between the Cl^- and Br^- -binding forms. This strongly suggests that the anion binding pocket accommodates Cl^- and Br^- , but not I^- or NO_3^- due to the larger size of the anions. It should be noted that the anion (Cl^- , Br^- , and NO_3^-) binding-induced difference spectra for NpHR show very similar spectral features (Fig. S7, ESI†), which are fully consistent with the previous results.¹⁵ Indeed, the intensity of anion-exchange-induced difference spectrum between each anion is smaller than that of the anion -minus- anion-free

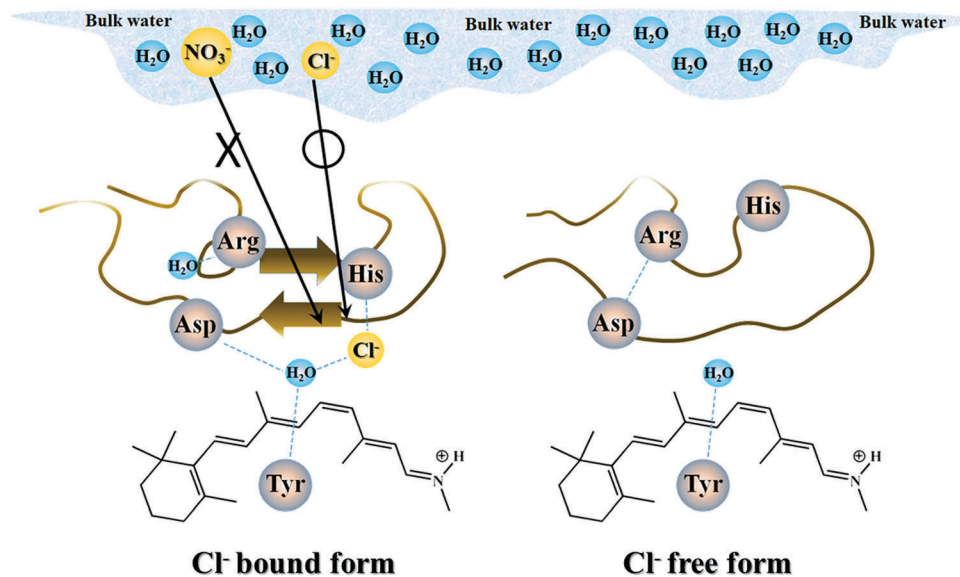


Fig. 4 Structural model of the Cl^- binding site of MG. (left) β -Sheet structure on the extracellular side is stabilized by binding of Cl^- . Four amino acids; His, Arg, Asp, and Tyr would be key residues for binding of Cl^- . (right) In the case of anion free form, the structure of the anion-binding site is flexible, resulting in the unfolding of the β -sheet structure.

spectra (Fig. S7, ESI[†]), which is contrary to the case of MG-pigment (Fig. 3). Perhaps, the obtained spectra in NpHR can be induced by the change of the electrostatic interaction with the retinal Schiff base rather than by perturbation of the anion binding site. In fact, it is reasonable to consider that the anions play a role as a counterion of the Schiff base in NpHR. Moreover, according to the crystal structures of NpHR, each anion is located in the vicinity of the retinal Schiff base with similar architecture around the anion binding site.³¹ Therefore, anion binding sites among L group pigments would be positively charged, where Cl^- (or Br^-) is accommodated for stabilization of the structure, which is contrary to the case for NpHR.

Fig. 4 illustrates the structural model for the anion binding site, which was constructed based on our experimental results. From the present study, it was elucidated that a chloride ion contributes to stabilization of β -sheet structure near the retinal binding pocket. The binding of Cl^- has been also known to stabilize the protonated Schiff base of the retinal chromophore in gecko P521 cone-type visual pigment by increasing the pK_a value.³² If the disruption of this electrostatic interaction between protonated Schiff base and counterion, Glu129, takes place in the absence of Cl^- , the retinal chromophore is released from the opsin moiety corresponding to thermal destabilization. Moreover, the β -sheet structure is stably located near the retinal binding pocket without binding of Cl^- in the case of rhodopsin as observed in the crystal structure.⁶ The amino acid identity around the retinal chromophore between rhodopsin and MG-pigment is about 40%; also, our previous light-induced difference FTIR spectra showed that the protein backbone structure and/or hydrogen bonding network, constituted by amino acid residues and internal water molecules, are significantly different from each other.^{7,8} Furthermore, the β -sheet specific amide-I band observed at 1620 cm^{-1} , which is a relatively low

frequency, indicates a stronger hydrogen-bonding structure than the original antiparallel β -sheet structure or probably a structure comprising intermolecular extended chains with water solvent. Therefore, we assumed that the β -sheet structure among L-group pigments possess their own structural motif.

In this study, we did not detect the vibrational signals of His and Lys, both of which play the role of a Cl^- binding site.⁴ Although C–N stretching vibration of His appears at $1000\text{--}900\text{ cm}^{-1}$ frequency region in general, it should be noted that the high concentration of phosphate (200 mM), used for suppression of protein swelling, obscures the His signal in the present study. Further, ATR-FTIR experiments with other buffer compositions or site-directed mutants of His will lead us to unveil the characteristic behavior of His upon the chloride binding. Moreover, according to the homology model of human green pigment, Lys200 side chain faces the outside from the putative Cl^- binding site.³³ Combined with the minor chloride effect of Lys mutation in λ_{max} ,⁴ Lys200 may influence stabilization of the chloride binding site indirectly rather than interacting directly with chloride. Thus, further spectral measurement of Lys200 mutants would reveal the local structural differences in the Cl^- binding site, particularly by focusing on the β -sheet specific amide-I band.

Conclusion

Binding of Cl^- to the L-group pigments alters the absorption spectra, and the molecular mechanism of the Cl^- effect was studied by applying ATR-FTIR spectroscopy to the MG pigment. The present study demonstrated that Cl^- -binding plays a critical role for stabilizing the secondary structure of the β -sheet, which protects the retinal binding pocket from the solvent on the extracellular side. Structural flexibility in the extracellular loop

region of animal rhodopsins allows a specific electrostatic interaction, leading to the absorbance of long wavelength light.

Methods

Pigment purification and ATR-ready sample preparation

The cDNA of monkey green (MG) pigment was tagged by the Rho1D4 epitope sequence and introduced into expression vector pcDLS α 296. This was expressed in the HEK293T cell line and regenerated with 11-*cis*-retinal as previously reported.^{7,8} The reconstituted pigment was extracted with buffer A [2% (w/v) *n*-dodecyl β -D-maltoside, 50 mM HEPES, 140 mM NaCl, and 3 mM MgCl₂ (pH 6.5)], purified by adsorption on an antibody conjugated column, and eluted with buffer B [0.06 mg mL⁻¹ 1D4 peptide, 0.02% *n*-dodecyl β -D-maltoside, 50 mM HEPES, 140 mM NaCl, and 3 mM MgCl₂ (pH 6.5)]. For the ATR-FTIR analysis, a solubilized sample was reconstituted into phosphatidylcholine liposomes with a 30-fold molar excess, followed by suspension in buffer C [2 mM phosphate and 10 mM NaCl (pH 7.25)].

ATR-FTIR measurements

The sample was placed on the surface of a diamond ATR crystal (nine internal total reflection). After it was dried in a gentle stream of N₂, the sample was rehydrated with solvent containing 200 mM phosphate (pH 7.25) buffer with 10 mM NaCl at a flow rate of 0.5 mL min⁻¹. ATR-FTIR spectra were first recorded at 2 cm⁻¹ resolution, using an FTIR spectrometer (Agilent, CA, USA) equipped with a liquid nitrogen-cooled MCT detector (an average of 1150 interferograms).^{21,34} After recording the FTIR spectrum in the second solvent without salt, the difference FTIR spectrum was calculated by subtracting the data obtained for the first and second solvents. The cycling procedure was repeated four to ten times, and the difference spectra were calculated as the averages of the presence -minus- absence spectra of salt. The spectral contributions of the unbound salt, the protein/lipid shrinkage and the water/buffer components were corrected.

Author contributions

K. K. and Y. F. designed most of the reported experiments. H. K. provided guidance throughout the investigations. K. K. and H. K. wrote the manuscript. K. K., Y. F., M. I., T. F., H. I. and H. K. advised on the experiments and manuscript preparation. K. K., M. I. and T. F. collected and analysed the data. All authors discussed the results of the paper.

Conflicts of interest

The authors declare no competing financial interests.

Acknowledgements

We thank Dr R. S. Molday for providing 293T cell lines and 1D4 antibodies. We also thank Mr S. Gulati for valuable discussion

and great helpful comments regarding this manuscript. This work was supported in part by grants from the Japanese Ministry of Education, Culture, Sports, Science and Technology to Y. F. (26640047 and 26708002), H. I. (16H01338, 15H05242 and 15H02421) and to H. K. (25104009, 15H02391).

References

- 1 T. Okano, D. Kojima, Y. Fukada and Y. Shichida, *Proc. Natl. Acad. Sci. U. S. A.*, 1992, **89**, 5932–5936.
- 2 J. L. Spudich, C. S. Yang, K. H. Jung and E. N. Spudich, *Annu. Rev. Cell Dev. Biol.*, 2000, **16**, 365–392.
- 3 O. P. Ernst, D. T. Lodowski, M. Elstner, P. Hegemann, L. S. Brown and H. Kandori, *Chem. Rev.*, 2014, **114**, 126–163.
- 4 Z. Wang, A. B. Asenjo and D. D. Orian, *Biochemistry*, 1993, **32**, 2125–2130.
- 5 J. A. Ballesteros and H. Weinstein, *Methods Neurosci.*, 1995, **25**, 366–428.
- 6 K. Palczewski, K. Kumasaka, T. Hori, C. A. Behnke, H. Motoshima, B. A. Fox, I. Le Trong, D. C. Teller, T. Okada, R. E. Stenkamp, M. Yamamoto and M. Miyano, *Science*, 2000, **289**, 739–745.
- 7 K. Katayama, Y. Furutani, H. Imai and H. Kandori, *Angew. Chem., Int. Ed.*, 2010, **49**, 891–894.
- 8 K. Katayama, Y. Furutani, H. Imai and H. Kandori, *Biochemistry*, 2012, **51**, 1126–1133.
- 9 Y. Furutani, Y. Shichida and H. Kandori, *Biochemistry*, 2003, **42**, 9619–9625.
- 10 K. Katayama, Y. Nonaka, K. Tsutsui, H. Imai and H. Kandori, *Sci. Rep.*, 2017, **7**, 4904–4914.
- 11 P. P. Rich and M. Iwaki, *Mol. Biosyst.*, 2007, **3**, 398–407.
- 12 Y. Furutani, H. Shimizu, Y. Asai, T. Fukuda, S. Oiki and H. Kandori, *J. Phys. Chem. Lett.*, 2012, **3**, 3806–3810.
- 13 H. Kandori, Y. Furutani and T. Murata, *Biochim. Biophys. Acta*, 2015, **1847**, 134–141.
- 14 S. Tachibanaki, Y. Imamoto, H. Imai and Y. Shichida, *Biochemistry*, 1995, **34**, 13170–13175.
- 15 J. Guijarro, M. Engelhard and F. Siebert, *Biochemistry*, 2006, **45**, 11578–11588.
- 16 T. Fukuda, K. Muroda and H. Kandori, *Biophysics*, 2013, **9**, 167–172.
- 17 T. Hirano, N. Fujioka, H. Imai, H. Kandori, A. Wada, M. Ito and Y. Shichida, *Biochemistry*, 2006, **45**, 1285–1294.
- 18 R. Takahashi and T. Noguchi, *J. Phys. Chem. B*, 2007, **111**, 13833–13844.
- 19 X. Hu, D. Kaplan and P. Cebe, *Macromolecules*, 2006, **39**, 6161–6170.
- 20 T. Morizumi, K. Sato and Y. Shichida, *Biochemistry*, 2012, **51**, 10017–10023.
- 21 Y. Kitade, Y. Furutani, N. Kamo and H. Kandori, *Biochemistry*, 2009, **48**, 1595–1603.
- 22 C.-H. Sung, B. G. Schneider, N. Agarwal, D. S. Papermaster and J. Nathans, *Proc. Natl. Acad. Sci. U. S. A.*, 1991, **88**, 8840–8844.

- 23 M. Matias-Florentino, R. Ayala-Ramirez, F. Graue-Wiechers and J. C. Zenteno, *Curr. Eye Res.*, 2009, **34**, 1050–1056.
- 24 I. Tsui, C. L. Chou, N. Palmer, C. S. Lin and S. H. Tsang, *Curr. Eye Res.*, 2008, **33**, 1014–1022.
- 25 J. M. Janz, J. F. Fay and D. L. Farrens, *J. Biol. Chem.*, 2003, **278**, 16982–16991.
- 26 M. Y. Liu, J. Liu, D. Mehrotra, Y. Liu, Y. Guo, P. A. Baldera-Aguayo, V. L. Mooney, A. M. Nour and E. C. Y. Yan, *J. Biol. Chem.*, 2013, **288**, 17698–17712.
- 27 J. Kleinschmidt and F. I. Harosi, *Proc. Natl. Acad. Sci. U. S. A.*, 1992, **89**, 9181–9185.
- 28 M. Shibata, N. Muneda, T. Sasaki, K. Shimono, N. Kamo, M. Demura and H. Kandori, *Biochemistry*, 2005, **44**, 12279–12286.
- 29 B. Hribar, N. T. Southall, V. Vlachy and K. A. Dill, *J. Am. Chem. Soc.*, 2002, **124**, 12302–12311.
- 30 T. Hirano, H. Imai, H. Kandori and Y. Shichida, *Biochemistry*, 2001, **40**, 1385–1392.
- 31 T. Kouyama, S. Kanada, Y. Takeguchi, A. Narusawa, M. Murakami and K. Ihara, *J. Mol. Biol.*, 2010, **396**, 564–579.
- 32 C. Yuan, O. Kuwata, J. Liang, S. Misra, S. P. Balashov and T. G. Ebrey, *Biochemistry*, 1999, **38**, 4649–4654.
- 33 R. E. Stenkamp, S. Filipek, C. A. G. G. Driessen, D. C. Teller and K. Palczewski, *Biochim. Biophys. Acta*, 2002, **1565**, 168–182.
- 34 Y. Furutani, T. Murata and H. Kandori, *J. Am. Chem. Soc.*, 2011, **133**, 2860–2863.